Paracrine effects of transplanted myoblasts and relaxin on post-infarction heart remodelling

Lucia Formigli [a], Avio-Maria Perna [b], Elisabetta Meacci [c], Lorenzo Cinci [a], Martina Margheri [a], Silvia Nistri [a], Alessia Tani [a], Josh Silvertown [d], Giovanni Orlandini [a], Cristina Porciani [e], Sandra Zecchi-Orlandini [a], Jeffrey Medin [d], Daniele Bani [a, *]

[a] Departments of Anatomy, Histology & Forensic Medicine, University of Florence, Florence, Italy
[b] Unit of Experimental Surgery, Careggi Hospital, Florence, Italy
[c] Department of Biochemical Sciences, University of Florence, Florence, Italy
[d] Ontario Cancer Institute, University Health Network, Toronto, Canada
[e] Unit of Cardiology, Careggi Hospital, Florence, Italy

Abstract

In the post-infarcted heart, grafting of precursor cells may partially restore heart function but the improvement is modest and the mechanisms involved remain to be elucidated. Here, we explored this issue by transplanting C2C12 myoblasts, genetically engineered to express enhanced green fluorescent protein (eGFP) or eGFP and the cardiotropic hormone relaxin (RLX) through coronary venous route to swine with experimental chronic myocardial infarction. The rationale was to deliver constant, biologically effective levels of RLX at the site of cell engraftment. One month after engraftment, histological analysis showed that C2C12 myoblasts selectively settled in the ischaemic scar and were located around blood vessels showing an activated endothelium (ICAM-1-,VCAM-positive). C2C12 myoblasts did not trans-differentiate towards a cardiac phenotype, but did induce extracellular matrix remodelling by the secretion of matrix metalloproteases (MMP) and increase microvessel density through the expression of vascular endothelial growth factor (VEGF). Relaxin-producing C2C12 myoblasts displayed greater efficacy to engraft the post-ischaemic scar and to induce extracellular matrix re-modelling and angiogenesis as compared with the control cells. By echocardiography, C2C12-engrafted swine showed improved heart contractility compared with the ungrafted controls, especially those producing RLX. We suggest that the beneficial effects of myoblast grafting on cardiac function are primarily dependent on the paracrine effects of transplanted cells on extracellular matrix remodelling and vascularization. The combined treatment with myoblast transplantation and local RLX production may be helpful in preventing deleterious cardiac remodelling and may hold therapeutic possibility for post-infarcted patients.

Keywords: myoblasts • relaxin • myocardial re-modelling • infarction • cell replacement therapy • C2C12 cells

Introduction

As injured cardiac tissue cannot regenerate, patients with ischaemic heart disease often develop heart failure. Since the onset of the concept of tissue engineering [1], therapeutic strategies aimed at improving myocardial function *via* local stem cell delivery, the so-called cellular cardiomyoplasty (CCM) are viewed as a promising strategy for the treatment of heart failure [2]. Different types of cells have been investigated, but only bone marrow-derived stem cells, endothelial progenitor cells and skeletal

*Correspondence to: Daniele BANI
Dept. Anatomy, Histology & Forensic Medicine
University of Florence, viale G.Pieraccini, 6
I-50139, Florence, Italy
Phone: (+39) 05 54 27 13 90, Fax: (+39)05 54 27 13 85
E-mail: daniele.bani@unifi.it*

myoblasts have been employed in clinical trials [3–5]. Despite the studies showing that functional benefits occur upon cell transplantation into the post-infarcted heart [2], enthusiasm for CCM has been recently tempered by controversy concerning the ability of the grafted cells to re-constitute myocardial tissue through trans-differentiation. Bone marrow stem cells are unable to diverge from their lineage restriction and adopt a cardiac phenotype [2, 5]. Skeletal myoblasts also exhibit little or no tendency to shift to a cardiac phenotype upon transplantation, as they typically differentiate to myotubes that remain embedded within the scar tissue, electrically and functionally isolated from the recipient heart [6]. These observations suggest that the observed benefits of CCM on heart contractility may depend on indirect, paracrine actions of the grafted cells on the post-infarcted heart, including angiogenesis and extracellular matrix remodelling [2, 7]. This assumption has gained support by recent findings that conditioned medium from mesenchymal stem cells contains pro-angiogenic factors and, when injected into the post-infarcted heart, exerts cardiac protection and induces functional recovery of the ischaemic myocardium [8]. Decreased collagen deposition and reduced scar stiffness of the post-infarcted myocardium can also contribute to the improvement of myocardial compliance and contractility observed after CCM [9], but the exact mediators responsible for these effects are still unknown. A potential approach to test this paracrine hypothesis is to combine cell therapy with regional expression of relaxin (RLX), a pleiotropic hormone best known for its extracellular matrix-re-modelling properties (10). RLX could be a good candidate, as it has multiple effects on the cardiovascular system, including coronary vasodilatation, neoangiogenesis, reduction of heart fibrosis and protection against myocardial ischaemia/reperfusion-induced injury [11–13].

Another key issue for the success of CCM is the route of cell administration. The most commonly used methods are the direct injection into the myocardium or trans-coronary venous implantation [5, 14]. However, these methods seem to favour the generation of clusters of grafted cells which may act as arrhythmogenic foci or produce myocardial embolization [15]. In contrast, cell delivery by retrograde venous route using intracoronary catheters offers several advantages over the other methods as it represents a safer method to allow a homogeneous settlement of the grafted cells into the post-infarcted myocardium [5, 16].

The current study was designed to expand knowledge on the potential mechanisms underlying the functional benefits of cell transplantation on the post-infarcted heart. C2C12 myoblasts, genetically engineered to express enhanced green fluorescent protein (eGFP) or eGFP and RLX were transplanted by retrograde coronary venous route to swine with chronic myocardial infarction. The object was to deliver constant, biologically effective levels of RLX at the site of cell engraftment. We also investigated the possible mechanisms involved.

Methods

Generation of C2C12 myoblast cell lines

Mouse skeletal C2C12 myoblasts (ATCC, Manassas, VA) were cultured in DMEM containing 10% foetal bovine serum (Sigma, Milan, Italy) Cells were transduced with a lentiviral vector bicistronically expressing human preprorelaxin 2 cDNA [17] and eGFP gene or just eGFP, under a cytomegalovirus (CMV) promoter and termed C2C12/RLX and C2C12/GFP, respectively. Day 2 supernatants from C2C12/RLX cell cultures contained 1.8 ± 0.2 ng/ml RLX, as assessed by a human H2 RLX-specific ELISA [17]. Clones were selected by cloning ring method and analysed by fluorescent microscopy and flow cytometry for eGFP expression.

Surgical treatments

The experimental protocol complied with the Declaration of Helsinki and the recommendations of the European Economic Community (86/609/CEE) on animal experimentation. Male swine, 30–40 kg, underwent ligation of the left anterior descending coronary artery after the 2nd diagonal branch to induce myocardial infarction, as previously described [13]. Thirty days after surgery, the animals were re-operated and a balloon catheter was inserted through the coronary sinus into the coronary vein draining the infarcted area to inject the myoblasts, either C2C12/RLX or C2C12/GFP (80×10^6 cells in 10–20 ml of culture medium), by retrograde venous route. Control animals were injected with cell-free culture medium. Cells or medium were injected over a 15-min period and the balloon catheter was kept inflated for further 20 min. to favour cell settlement. All the

transplanted animals underwent daily administration of cyclosporine (1 mg/ kg b.wt.) and betamethasone (0.1 mg/kg b.wt.) to obtain immune-suppression and anti-inflammatory effects to enhance grafting chances of the heterologous cells. The same treatment was also administered to the untransplanted controls. They were housed for a further 30 days and then sacrificed. At autopsy, cardiac tissue samples taken 1–2 cm downstream the coronary occlusion were taken for biochemical and morphological analyses. Overall, mortality upon induction of myocardial infarction was about 30%. The experiment was terminated when each group comprised five animals. The levels of RLX yielded by the above cell grafting protocol were measured in plasma, isolated from peripheral blood, and cardiac tissue extracts taken at sacrifice from swine injected with C2C12/RLX using a commercial human H2 RLX ELISA kit (Immundiagnostik, Bensheim, Germany). Untransplanted swine and animals receiving C2C12/GFP were used as controls. To this end, the tissue samples, 50 mg each, were minced and homogenized in cold lysis buffer composed by (mmol/l): Tris/HCl pH 7.4 10, NaCl 10, $MgCl_2$ 1.5, Na_2EDTA 2, phenylmethylsulfonyl fluoride (PMSF) 1, Triton X-100 (1%), Leupeptin (20 µg/ml), Pepstatin (1 µg/ml), Pefabloc (1 mg/ml), Aprotinin (2.5 µg/ml). Upon centrifugation at 13,000 g for 10 min. at 4°C, the supernatants were collected and kept frozen at -20°C until needed.

Confocal immunofluorescence

Cryostat sections, 10 µm thick, were cut from frozen tissue samples, fixed in paraformaldehyde vapours for 10 min. and incubated with the following antibodies: rhodamine-conjugated mouse monoclonal anti-eGFP (Santa Cruz, CA; 1:200); mouse monoclonal anti-α sarcomeric actin (Dako, Milan, Italy; 1:100); rabbit polyclonal anti-VCAM-1 (Santa Cruz; 1:100); mouse monoclonal anti-ICAM-1 (Chemicon, Temecula, CA; 1:200). When needed, immune reaction was revealed by Alexa 488-conjugated antimouse or antirabbit secondary antibodies (1:50; Molecular Probes, Eugene, OR). Negative controls were performed with non-immune mouse serum substituted for the primary antibody. Cells were examined with a Bio-Rad 1024 confocal laser scanning microscope (Bio-Rad, Hercules, California, USA) equipped with a Krypton/Argon laser for fluorescence measurements and differential interference contrast optics for transmission images. Series of optical sections at intervals of 0.4 µm were taken and superimposed as a single image. In each animal, GFP-positive cells were counted on five microscopical fields, 32,400 µm^2, containing at least one vascular profile. The numbers from two different observers were then averaged.

Ultrastructure of cardiac tissue

Cardiac tissue samples were fixed in glutaraldehyde-osmium tetroxide, embedded in epoxy resin and routinely processed for transmission electron microscopy. Some fragments, not osmium-fixed, were used for immunoelectron microscopy to detect RLX in the grafted C2C12/RLX cells. Ultra-thin sections were etched with 30% hydrogen peroxide and incubated with normal goat serum (Sigma; 1:20) to quench non-specific binding sites, then with rabbit polyclonal anti-H2 RLX antibodies (Immundiagnostik; 10 µg/ml) and finally with goat antirabbit antibodies conjugated with 5 nm colloidal gold particles (BBInternational, Stanstead, UK; 1:20). Negative controls were sections in which non-immune rabbit serum was substituted for the primary antiserum. The sections were counterstained with uranyl acetate and lead citrate and examined under a Jeol 1010 (Jeol, Tokyo, Japan) electron microscope at 80 kV.

Determination of fibrosis

Fibrosis in the cardiac scar was studied by qualitative and quantitative morphological methods on paraformaldehyde-fixed, paraffin-embedded samples. Sections 8 µm thick were stained with Van Gieson method for collagen (fuchsin 0.1% in H_2O containing 0.08% HCl for 4 min., followed by 5-min. rinsing in 95% ethanol). Five microscopical fields per animal were registered by a digitizing camera applied to a light microscope with a 20 x objective, each field corresponding to a test area of 141,100 µm^2. On the digitized images, measurements of overall surface area (SA) and optical density (OD) of the collagen fibres were carried out using the Scion Image Alpha 4.0.3.2 image analysis program (Scion Corp., Frederick, Maryland, USA), upon appropriate threshold to exclude amorphous ground substance. For each animal, a sclerosis index was calculated by the formula: SA x OD x 10^{-6}. Values from the five animals in each group were then averaged.

Matrix metalloprotease activity in cardiac tissue and C2C12 myoblasts

Assay for matrix metalloprotease (MMP)/collagenase activity was performed by gelatin zymography assay. Primary cultures of cardiac cells from the post-infarcted scar were obtained by incubating the minced tissue with collagenase II (250 IU/ml) in Hank's balanced salt solution, pH 7.4, for 40 min. at 37°C. Cells were filtered, plated in DMEM growing medium on 12-well multiplates and used at passages 0–1. By this procedure, the cells obtained were mainly

fibroblasts and endothelial cells (data not shown). The cardiac cells were co-cultured with myoblasts (C2C12/RLX or C2C12/GFP) for 72 hrs in serum-free DMEM at a approx. 3:1 ratio. As controls, primary cardiac cells treated or not with 1.8 ng/ml recombinant H2 RLX (Connetics Co., Palo Alto, California, USA), and subconfluent C2C12/RLX and C2C12/GFP cells were analysed after 72 hrs culture. The conditioned medium was then collected and centrifuged at 10,000 x g for 15 min. In some experiments zymography assay was performed on lysates obtained from the post-infarcted myocardium of control and transplanted animals. The tissue was homogenized in cold buffer containig 5 mM Tris-HCl, 320 mM sucrose, 1 mM dithiothreitol, 10 µg/ml leupeptin, 10µg/ml soybean inhibitor, 2 µg/ml aprotinin. Tissue homogenates were centrifuged at 10,000 rpm for 10 min. at 4°C and then the supernatant used for zymography assay. Protein content was measured in cell and tissue lysates by the bicinchoninic acid method. Samples of conditioned medium, 10 µl each, or of tissue (150 µg) were mixed with sample buffer (0.03% bromophenol blue, 0.4 mol/l Tris-HCl pH 7.4, 20% glycerol, 5% SDS) and separated on 10% SDS-polyacrylamide gels containing gelatin (1 mg/ml). After electrophoresis, gels were washed for 1 hrs in re-naturation buffer (2.5% Triton X-100 in bidistilled water) and subsequently incubated for 4 hrs at 37°C in 50 mmol/l Tris, 200 mmol/l NaCl and 5 mmol/l CaCl$_2$, pH 7.5. Gels were stained with 0.05% Coomassie Brilliant Blue and destained with 30% methanol and 10% acetic acid; clear zones within the background indicated proteolytic activity. MMPs were identified by comparison with the respective recombinant protein (Calbiochem-Novabiochem) and molecular weight standards. Quantification was performed by densitometry (QuantityOne software, Bio-Rad).

Determination of microvessel density

The volume density of microvessels in the cardiac scar tissue was measured by point counting on semi-thin sections of resin-embedded samples. Ten microscopical fields per animal were registered by the same device described above using a 20 x objective. A single square grid, with distance between intersection points = 30 µm on the section, was superimposed on each image. Test points corresponding to the SA of microvessels were then counted. Measurements performed by two independent observers were averaged.

VEGF expression in cardiac tissue

VEGF gene expression in the post-infarcted myocardium were investigated on frozen samples by reverse transcription-PCR (RT-PCR). Total RNA was extracted from homogenized tissue using Trizol (Gibco-BRL) and quantified spectrophotometrically at 260-nm wavelength. Total RNA (700 µg) was reverse-transcribed and amplified with SuperScript One-Step™ RT-PCR System (Invitrogen, Groningen, NL). cDNA was synthesized for 30 min. at 55°C, pre-denatured for 2 min. at 94°C and subjected to 35 cycles of PCR performed at 94°C for 15 sec., 57.3°C for 30 sec. and 72°C for 1 min.; the final extension step was performed at 72°C for 5 min. Internal standards were generated by amplifying β-actin mRNA (annealing temperature: 55°C). The following primers were used: mouse VEGF (GenBank: M95200.1): forward 5'-CAGGCTGCTGTAAC-GATGAA-3', reverse 5'-TTTCTCCGCTCTGAACAAGG-3'; porcine VEGF (GenBank: NM_214084.1): forward 5'-AGGAGTACCCCGATGAGATC-3', reverse 5'-GGGATTTT-CTTGCCTCGCTC-3'; porcine β-actin (GenBank: NM_031144): forward 5'-CCAACCGTGAAAAGATGACC-3', reverse 5'-AGAGGTCTTTACGGATGTCA-3'. Expected length of amplified fragments were 202, 200 and 539 base pairs for mouse VEGF, porcine VEGF and β-actin, respectively. PCR products were electrophoresed on a 2% agarose gel and stained with ethidium bromide.

Assessment of cardiac function

To evaluate ventricular contractile function, the animals underwent trans-thoracic Doppler echocardiography using a Philip EN/Visor C echocardiograph equipped with a 3.5 MHz phased array transducer. Analysis was carried out at 3 time points: before surgery; 1 month after myocardial infarction immediately prior to cell injection; 1 month after cell transplantation. The following parameters were evaluated: left ventricular end-diastolic and end-systolic diameters (LVEDD and LVESD; expressed as mm), ejection fraction (EF; expressed as percentage), according to Simpson's method, and myocardial performance index (MPI), calculated as the ratio between the sum of isovolumetric contraction and relaxation times and the ejection time [18, 19].

Statistical analysis

Values are means ± SEM of the five animals per group. Unless otherwise stated, differences between the experimental groups were evaluated by one-way ANOVA and Newman-Keuls post-test. Calculations were made with Prism 4 (GraphPad, San Diego, CA) statistical program.

Results

Morphological analysis of myoblast homing to the post-infarcted myocardium

By confocal immunofluorescence, numerous GFP-immunoreactive cells, either C2C12/GFP or

Fig. 1 (**A–D**) Merged confocal fluorescence and differential interference contrast images of sections from control (**A**), C2C12/GFP-transplanted (**B**) and C2C12/RLX-transplanted (**C, D**) hearts. Sections were stained with anti-GFP antibodies (red) to identify the engrafted myoblasts and counterstained with Syto3 (green) to reveal nuclei (**A–C**). In (**D**), the sections were stained with antibodies against the skeletal muscle-specific isoform of a-sarcomeric actin. Myoblast-injected hearts show immunoreactive cells in the post-infarcted zone (**B–D**), mainly located around blood vessels (asterisks) and scattered within the extracellular matrix. No labelled cells can be detected in the controls. C2C12/RLX-implanted hearts contain significantly more GFP-immunoreactive cells than the C2C12/GFP-implanted ones. (**E–G**) Confocal micrographs of sections from C2C12/RLX-treated hearts, immunostained for V-CAM (**E**) and ICAM (**F, G**). Both molecules (green) are expressed by endothelial cells of microvessels in the post-infarcted zones (**E, F**); by contrast, no ICAM staining is observed in the surrounding viable myocardium. Nuclei are counterstained with propidium iodide (red). Bars = 20 μm.
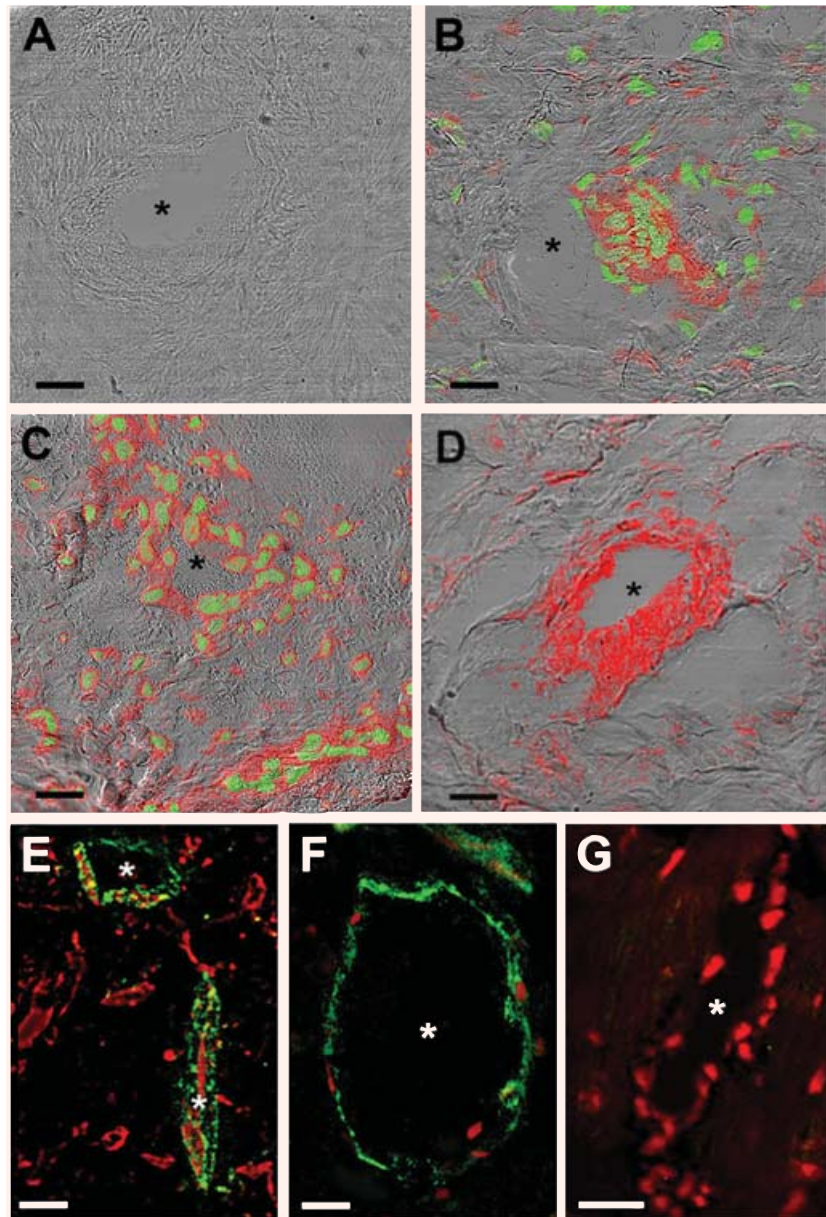
C2C12/RLX, were found in the scar tissue from the transplanted groups but not in the control group (Fig. 1A–C). Their myoblastic nature was confirmed by positive staining for a sarcomeric actin (Fig. 1D). C2C12/GFP-injected hearts contained a lower number of immunoreactive cells compared with C2C12/RLX-injected hearts (40 ± 7 *versus* 83 ± 12 cells/microscopical field; Student's t-test: *P*<0.01). The engrafted cells were preferentially located around blood vessels or in their close proximity and were almost absent in the peri-infarcted, viable myocardium. Interestingly, a clear-cut endothelial expression of ICAM-1 and VCAM (Fig. 1E and F) was detected in small-sized blood vessels within the post-infarcted zone, but not in the non-ischaemic myocardium (Fig. 1G), suggesting a role for activated endothelium of the injured regions in myoblast extravasation and homing. Immunoelectron microscopy of hearts transplanted with C2C12/RLX revealed the presence of RLX-producing cells in the
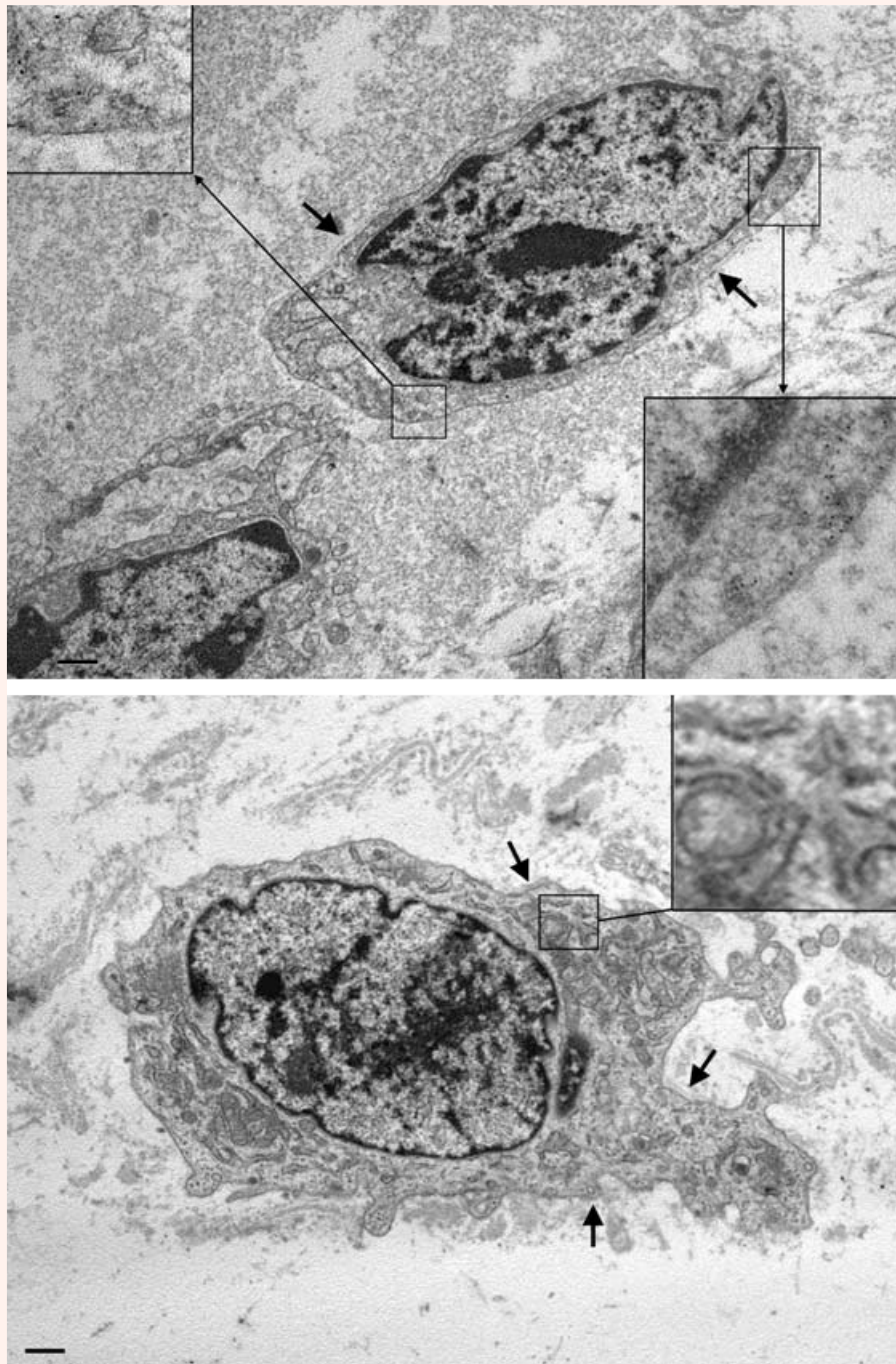
Fig. 2 Immunoelectron micrographs of C2C12 myoblasts grafted in the post-infarcted heart, immunostained with anti-RLX antibodies (revealed by 5 nm gold particles). In the upper panel, a C2C12/RLX myoblast shows clear-cut cytoplasmic RLX immunoreactivity (details in the insets). In the lower panel, a C2C127GFP myoblast shows no immunolabelling (detail of the RER area in the inset). Both cells show a discontinuous basement membrane (arrows) and are surrounded by a loose extracellular matrix. Bar = 0.5 μm.

Fig. 3 *Upper panels.* Light micrographs of sections from control (**A**), C2C12/GFP- (**B**) and C2C12/RLX-transplanted hearts (**C**), stained with Van Gieson for collagen. A marked reduction of the extent of fibrosis can be seen in the ischaemic scars of the myoblast-transplanted hearts; of note, fibrosis is particularly attenuated in the hearts receiving C2C12/RLX cells. Bar = 20 μm. *Centre panel.* Sclerosis index (optical x volume density of collagen fibres) in the post-infarcted myocardium, estimated by computer-aided morphometry; (**a**) *P*<0.05 *versus* controls; (**b**) *P*<0.001 *versus* controls; (**c**) *P*<0.001 *versus* C2C12/GFP. *Lower panels.* Electron micrographs of fibroblasts from control (**D**) C2C12/GFP- (**E**) and C2C12/RLX-transplanted hearts (**F**). In the control, collagen microfibrils form large bundles adjacent to the cell's plasma membrane (inset), as occurs during *de novo* fibre assembly; in the C2C12/GFP-transplanted hearts, and even more in the C2C12/RLX-transplanted ones, collagen microfibrils are scattered and loosely arranged. Bar = 0.5 μm.
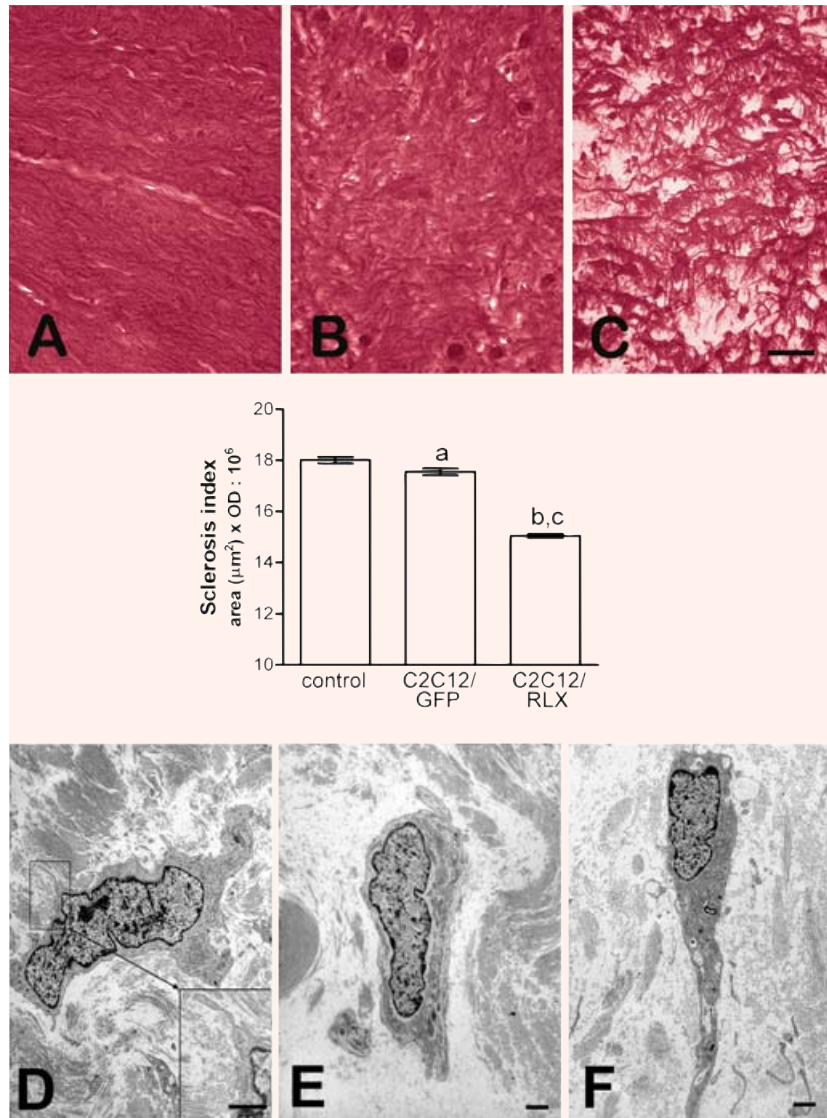
post-infarction area, containing RLX gold labelling (Fig. 2). As expected, RLX-immunoreactive cells were not found in the hearts transplanted with C2C12/GFP (Fig. 2). The engrafted myoblasts could be distinguished by the activated fibroblasts in the scar because they showed a discontinuous basement membrane and lack collagen microfibrils apposed to the plasma membrane typical of fibroblasts (compare with Fig. 3D). However, the injected myoblasts remained single elements with no tendency to fuse into multinucleated myotubes, which were never observed in the scar tissue (Figs. 1 and 2). This finding suggests that C2C12 myoblasts are unable to

regenerate contractile tissue at the grafting site, at least in the current experimental conditions.

Extracellular matrix remodelling and microvessel density in the post-infarcted myocardium

By Van Gieson staining, collagen fibres markedly accumulated in the post-infarcted myocardium of the control animals and were reduced in the transplanted groups, especially in C2C12/RLX-treated animals (Fig. 3A and C). Notably, ventricular tissue samples
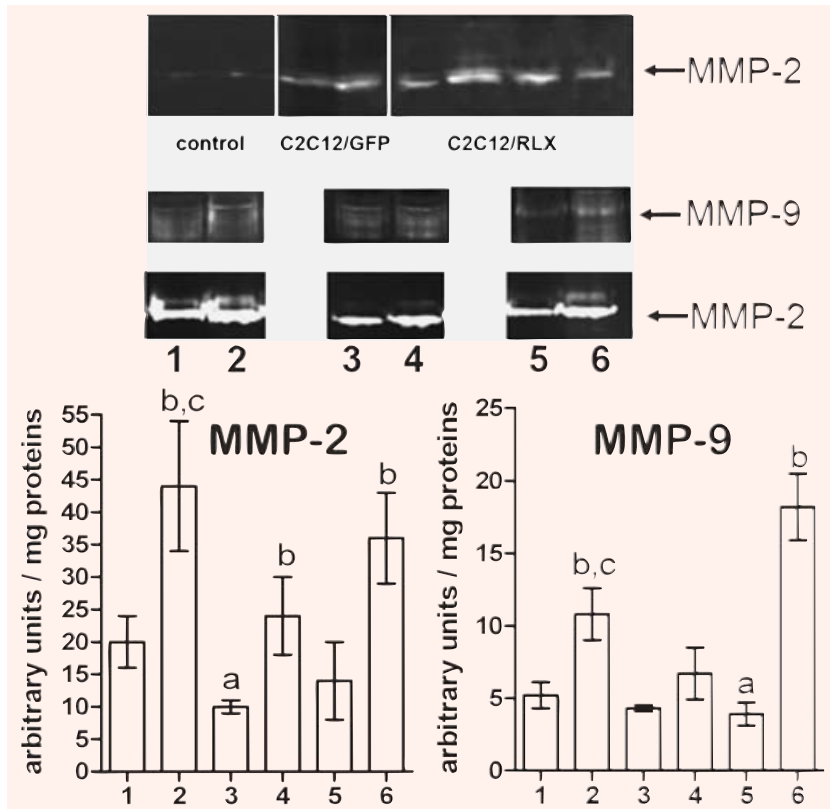
Fig. 4 *Upper panel.* Matrix metalloprotease (MMP) activity evaluated by gelatin zymography on cardiac tissue samples from control (n=2, optical density: 36±1), C2C12/GFP-transplanted (n=2, optical density: 92±4) and C2C12/RLX-transplanted swine (n=4, optical density: 106±13). *Centre and lower panel.* MMP activity on conditioned media from: primary cultures of swine cardiac cells co-cultured with C2C12/GFP (1) or C2C12/RLX myoblasts (2), primary cultures of swine cardiac cells incubated with medium (3) or with H2 RLX (4), C2C12/GFP (5) and C2C12/RLX myoblasts (6). Densitometric analysis of MMP activity, expressed as arbitrary optical density units normalized to protein content. Molecular weights of the collagen lysis bands are consistent with MMP-9 and MMP-2. Transfection or treatment with RLX preferentially up-regulated MMP 2 activity. (**a**), *P*<0.05 *versus* the co-cultures of cardiac cells and C2C12/GFP; (**b**) *P*<0.05 *versus* the counterparts without RLX; (**c**) *P*<0.05 *versus* cardiac cells treated with exogenous RLX.

coming from the post-infarcted areas were very similar in histological appearance among the animals of each group. Morphometric analysis of tissue collagen content confirmed the visual observation (Fig. 3). By electron microscopy, fibroblasts from the control hearts featured activated cells, with cytoplasms filled with protein synthesizing organelles and surrounded by collagen bundles (Fig. 3D). Conversely, in the hearts receiving C2C12/RLX, fibroblasts were immersed in a loose extracellular matrix with few, thin collagen fibrils (Fig. 3E). We then analysed MMP/collagenase activity in tissue homogenates from the post-infarction scar, as well as in primary cultures of swine cardiac cells incubated together with C2C12/GFP or C2C12/RLX. MMP-2 activity was very low in the control hearts, whereas it was significantly increased in the hearts containing grafted C2C12/GFP and C2C12/RLX cells (*P*<0.01). We also observed a tendency of C2C12/RLX-grafted hearts to possess higher MMP-2 activity compared to the C2C12/GFP ones, although the differences did not reach statistical significance. On the other hand, we found that both the co-cultures released collagen-degrading enzymes in the supernatants, with significantly higher levels in those containing C2C12/RLX cells (Fig. 4). Of interest, both resident cardiac cells and myoblasts contributed to MMP activity and this effect was significantly enhanced by exogenous or endogenous RLX (Fig. 4). Finally, we studied scar tissue vascularization. In C2C12/GFP-transplanted hearts, microvessel density was slightly but significantly increased compared to the control group, while it reached the highest values in C2C12/RLX transplanted hearts (Fig. 5). Interestingly, changes in microvascular density paralleled with porcine VEGF mRNA expression in the cardiac scar (Fig. 5). Indeed, VEGF mRNA was absent in control hearts, absent or only slightly expressed in C2C12/GFP-injected hearts and well detectable in the C2C12/GFP-injected hearts (Table 1). On the other hand, C2C12-derived mouse VEGF transcript was not detected in the specimens from transplanted animals (data not shown), suggesting that the engrafted myoblasts do not play a substantial contribution to local VEGF production.

Fig. 5 *Upper and centre panels.* Light micrographs of the microvascular network in control (**A**), C2C12/GFP- (**B**) and C2C12/RLX-transplanted hearts (**C**), and morphometric assessment of microvascular density. Both C2C12/GFP- and C2C12/RLX-injected hearts exhibit higher microvascular density than the control hearts. Of note, C2C12/RLX-injected hearts show significantly higher microvascular density than C2C12/GFP-injected ones. (**a**) *P*<0.05 *versus* control; (**b**) *P*<0.01 *versus* control; (**c**) *P*<0.05 *versus* C2C12/GFP. *Lower panel.* RT-PCR assay for porcine VEGF transcripts in scar tissue samples from controls (lanes 1, 2), C2C12/GFP- (lanes 3,4) and C2C12/RLX-transplanted hearts (lanes 5, 6). Images are representative of five different animals per experimental groups. Porcine VEGF mRNA is absent in the control samples, is slightly expressed in one of the two samples of C2C12/GFP-injected hearts, and clearly detectable in both the samples from C2C12/RLX-injected hearts.
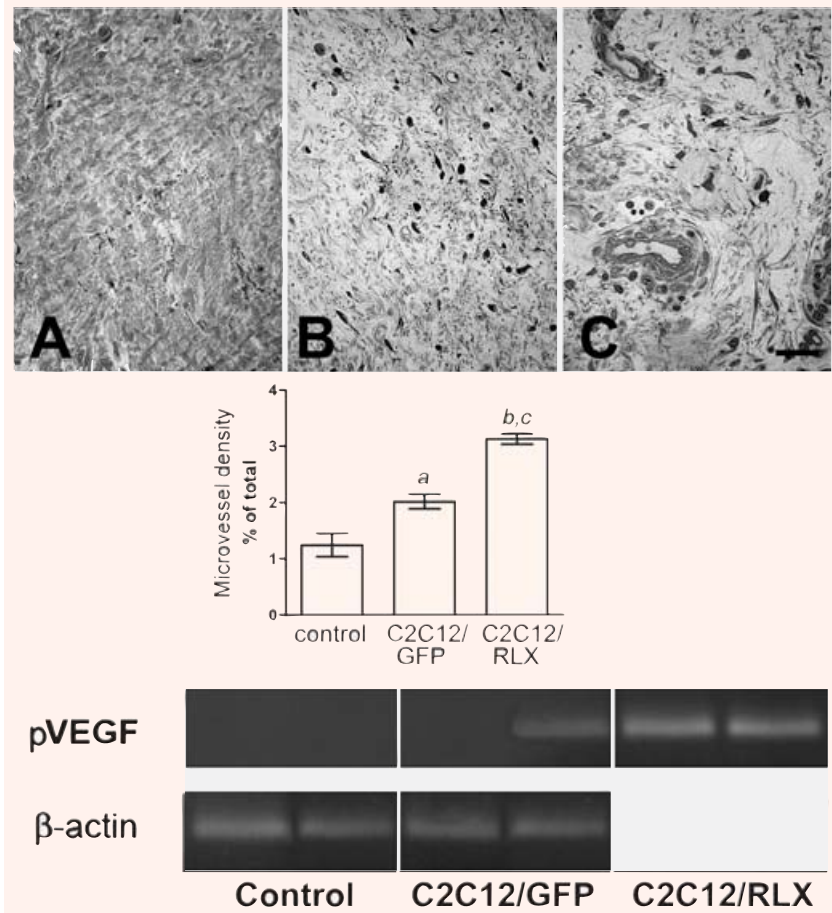
Table 1 VEGF mRNA expression in post-infarction cardiac scar tissue

Animal No.	Controls	C2C12/GFP	C2C12/RLX
1	-	-	++
2	-	+	+++
3	-	-	++
4	-	-	+++
5	-	-	+

Semi-quantitative evaluation of the intensity of the bands of RT-PCR amplicons for porcine VEGF.

Plasma and cardiac tissue levels of RLX

By a specific ELISA assay for H2 RLX, no detectable levels of the hormone were found in either blood or tissue samples from untransplanted controls and C2C12/GFP-treated animals. In the swine given C2C12/RLX myoblasts, RLX was detected, although at very low levels (85±12.3 pg/ml), in the post-infarcted cardiac tissue but not in blood.

Cardiac function after cell transplantation

We finally investigated whether myoblast grafting could improve the heart contractile performance by Doppler echocardiography. Under basal conditions, the animals of all groups showed similar values of MPI, EF and left ventricular diameters (Fig. 6). One month after myocardial infarction, the post-infarcted area had a comparable extension in all the animal groups and involved anteroseptal mid and apical segments. Paradoxical motion occurred in two animals, whereas akinesia was observed in all the remaining animals. MPI, which is inversely related to ventricular functional impairment, as well as LVEDD
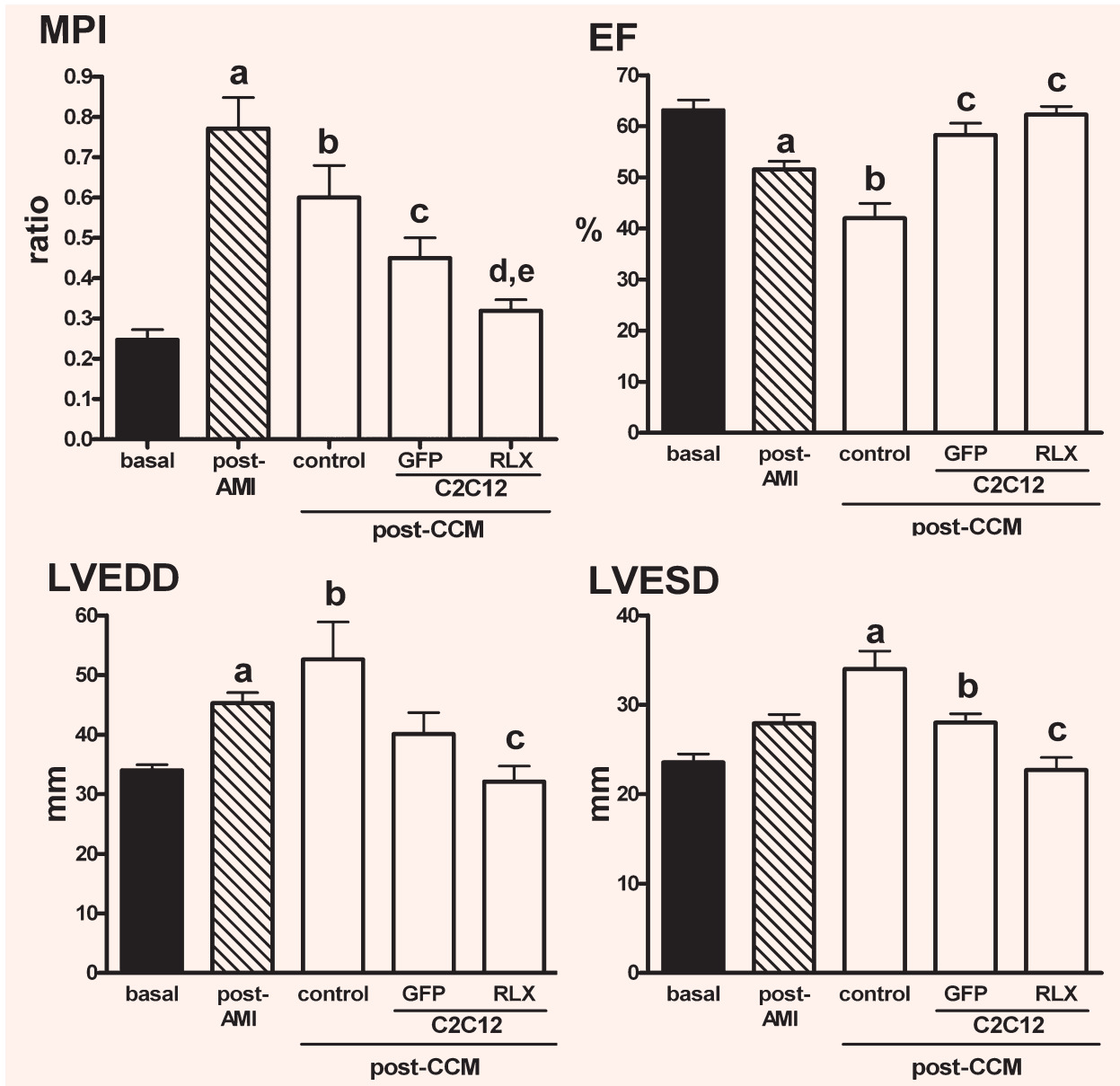
Fig. 6 Myocardial performance index (MPI), ejection fraction (EF), left ventricular end-diastolic and end-systolic diameters (LVEDD, LVESD) evaluated in basal conditions (black bars), 1 month after the induction of myocardial infarction (post-AMI; striped bars) and 1 month after cell transplantation (post-cellular cardiomyoplasty [CCM]; open bars). Myoblast implantation improves cardiac function. C2C12/RLX myoblasts are more effective than C2C12/GFP ones. Significance of differences (one-way ANOVA): MPI: (**a**) $P<0.001$ *versus* basal; (**b**) $P<0.001$ *versus* post-AMI; (**c**) $P<0.01$ *versus* controls; (**d**) $P<0.001$ versus controls; (**e**) $P<0.05$ *versus* C2C12/GFP. EF: (**a**) $P<0.01$ *versus* basal; (**b**) $P<0.001$ *versus* post-AMI; (**c**) $P<0.001$ *versus* controls. LVEDD: (**a**) $P<0.05$ *versus* basal; (**b**) $P<0.01$ *versus* basal; (**c**) $P<0.01$ *versus* controls. LVESD: (**a**) $P<0.01$ *versus* basal & post-AMI; (**b**) $P<0.05$ *versus* controls; (**c**) $P<0.001$ *versus* controls.

and LVESD were markedly increased, whereas EF was significantly decreased compared with the basal values (Fig. 6). One month after cell transplantation, MPI was markedly improved, EF was increased and LVEDD and LVESD were slightly reduced in both the transplanted groups as compared with the controls.

Notably, MPI in C2C12/RLX-treated hearts was significantly lower than in the C2C12/GFP-treated group, whereas the other parameters assayed were also improved, although the values did not reach statistical significance with only five animals per group (Fig. 6). Collectively, these data indicate that implanted C2C12 cells attenuated ventricular dysfunction after myocardial infarction and suggest that C2C12/RLX cells are more effective in improving cardiac performance.

Discussion

The present study has shown that transplanted skeletal myoblasts produce increased vascularization, promote collagen turnover and reduce fibrosis, thereby improving left ventricular function. These effects appear more prominent when myoblasts over-expressing RLX were used. This study has also underlined the importance of paracrine effects of grafted cells in explaining cardiac functional improvement and demonstrates the efficacy of retrograde venous injection of cells in a large animal model that fairly reproduces the human clinical conditions [5]. This study confirms previous findings with myoblasts with one major difference; the myoblasts were injected 1 month after the induction of myocardial infarction, thus reproducing a more likely clinical scenario than the injection of cells immediately after injury, as done in most previous studies [2–4].

The use of transplanted cells over-producing cardiotropic factors is particularly relevant in consideration of the healing mechanisms involved in the post-infarcted heart, which include a cascade of interwoven events such as inflammation, cardiomyocyte demise and formation of fibrous scar [20]. These changes increase the mechanical and functional stress on the heart resulting in deterioration of cardiac performance and deleterious ventricular remodelling. Recently, stem cell-based myocardial regeneration has been viewed as a potential therapeutic tool for post-ischaemic dysfunction and many studies have claimed improved cardiac function and attenuation of adverse remodelling upon CCM (2–5). Theoretically, two distinct mechanisms might be involved in the ability of the grafted cells to sustain cardiac contraction: trans-differentiation of progenitor cells into myocardial and/or vascular tissues and

secretion of soluble factors exerting paracrine effects on the host tissue. We show here that myoblast transplantation improves the function of post-infarcted hearts through paracrine pathways, consisting mainly in attenuation of collagen fibre deposition and increase in the microvascular network in the ischaemic scar. The functional benefits of myoblast transplantation, especially using genetically engineered RLX-producing cells, were properly shown by the improvement of the echocardiographic indexes and parameters of cardiac performance observed in the transplanted animals. In particular, the utility of MPI in predicting left ventricular functional outcome has been demonstrated in a large cohort of patients with myocardial infarction [21] and it has been shown to closely reproduce functional contractile parameters measured using invasive catheter-based methods [18, 19].

The present findings confirm and extend the results from previous studies on the ability of transplanted cells to exert pro-angiogenetic and cardioprotective actions on the ischaemic myocardium and contribute to the idea that other mechanisms independent of myocardial trans-differentiation may improve cardiac function [8, 22]. In particular, we found that injection of C2C12 myoblasts *via* the retrograde venous route in post-infarcted swine hearts provided a selective dissemination of the cells within the injured tissues. Since these cells were mainly located around small blood vessels showing a permissive endothelium (*i.e.* expressing endothelial adhesion molecules such as ICAM-1 and VCAM), we suggest that factors controlling the inflammatory process in the post-infarcted myocardium [23] may also guide myoblast extravasation from the blood. Indeed, it has been previously shown that circulating stem cells selectively migrate to the ischaemic regions of the heart [24]. In our study, the engrafted myoblasts failed to trans-differentiate into contractile myocardium, in keeping with previous reports [6]. Instead, their presence within the fibrotic area was associated with a remarkable loosening of the extracellular matrix and increase in tissue microvascular density, indicating that these cells were able to modify the elastic and trophic properties of the post-infarcted myocardium. Noteworthy, the concept of using myoblasts as carriers for RLX provided additional benefits to the post-infarction repair compared with myoblasts alone, due to the superior ability of C2C12/RLX to engraft the ischaemic hearts, re-model

collagen and affect microvessel behaviour. This is in agreement with previous studies showing that RLX is a potent anti-fibrotic agent, capable to reduce the extent of fibrosis and induce extracellular matrix remodelling in various organs, including the heart [10, 12, 25]. The use of RLX-producing cells may have some advantages over the use of exogenously administered RLX, consisting mainly in the possibility to obtain local, constant and biologically effective levels of this hormone in the remodelling heart. In this way, RLX may synergize with other paracrine factors released *in situ* by the grafted myoblasts. Changes in extracellular matrix composition in the evolving infarction may change the physical properties of the scar and lead to better ventricular compliance reduced myocardial stress and overall improvement of cardiac function. Several lines of evidence converge towards this interpretation: (*i*) mesenchymal cell injection into acute ischaemic myocardium reduces ventricle dilatation affecting the fibrotic microenviroment and elastic properties of the infarcted area [9]; (*ii*) inhibition of monocyte chemoattractant protein-1 attenuates post-infarction myocardial failure by decreasing cardiac fibrosis [26]; and (*iii*) skeletal myoblasts infused into the injured myocardium elicit collagen remodelling within the infarcted zones [16]. Increased microvessel density in the post-infarcted cardiac scar may provide additional benefits to matrix re-modelling, contributing to the creation of a more favourable microenviroment capable of improving grafted cell survival, reducing scar stiffness and preventing cardiomyocyte apoptosis in the peri-infarction myocardium. This may also contribute to explain the higher number of engrafted C2C12/RLX compared with the C2C12/GFP observed in the present study. However, a direct role of RLX in sustaining cell viability cannot be ruled out, but this issue would require additional study.

It has to be pointed out that, in our study, grafting of C2C12/RLX myoblasts did not result in detectable circulating levels of RLX, thus leading us to exclude possible systemic effects of this hormone. Of note, RLX has been reported to have significant angiogenic and anti-fibrotic effects only in diseased organs and tissues, leaving normal targets unaffected [27, 28].

The paradigm of a paracrine protection of post-infarcted myocardium by the grafted cells is further supported by the observation that C2C12/GFP myoblasts and more effectively C2C12/RLX cells were able to up-regulate MMP activity and VEGF expression in cardiac cells. MMPs are involved in extracellular matrix turnover, both in physiological conditions or in response to inflammatory stimuli [29]. They also play a role in myoblast migration and fusion during muscle development and regeneration [30], inflammatory cell invasion of the infarcted myocardium during early healing [31], and post-infarction ventricle re-modelling and dilatation [32]. On this basis, MMP activation and subsequent attenuation of scar stiffness may also explain the greater engraftment potential of C2C12/RLX myoblasts as compared with C2C12/GFP.

VEGF is a key promoter of angiogenesis and has a straightforward role in CCM. In fact, VEGF gene transfer enhances the efficacy of CCM in animal models of chronic myocardial infarction [33, 34], and intramyocardial injection of mesenchymal stem cells results in up-regulation of tissue VEGF expression associated with improved cardiac perfusion and contractility [35]. In our study, the levels of VEGF transcripts in the cardiac scar correlated well with the grade of microvascular density, as it was higher in C2C12/RLX-injected hearts which showed a more extended vascular network. These findings are consistent with the known vascular properties of RLX, capable to induce coronary vasodilatation, sustain coronary flow, and induce *de novo* angiogenesis and VEGF expression [11, 25, 27].

In conclusion, our study suggests that the improvement of cardiac function after myoblast transplantation into post-infarcted myocardium mainly relies on paracrine actions of the donor cells rather than on myocardial trans-differentiation. These effects appear to depend on local diffusible factors, namely MMP and VEGF, capable to influence stiffness and vascularization of the ischaemic scar. It also suggests that genetically modified, RLX-producing cells can behave as an intrinsic RLX source in the ischaemic myocardium capable to substantially improve the benefits of myoblast transplantation.

Grants

References

1. **Vacanti CA.** The history of tissue engineering. *J Cell Mol Med.* 2006; 10: 569–76.

2. **Rubart R, Field LJ.** Cardiac regeneration: repopulating the heart. *Annu Rev Physiol.* 2006; 68: 29–49.

3. **Walter DH, Haendeler J, Reinhold J, Rochwalsky U, Seeger F, Honold J, Hoffmann J, Urbich C, Lehmann R, Arenzana-Seisdesdos F, Aicher A, Heeschen C, Fichtlscherer S, Zeiher AM, Dimmeler S.** Impaired CXCR4 signaling contributes to the reduced neovascularization capacity of endothelial progenitor cells from patients with coronary artery disease. *Circ Res.* 2005; 97: 1142–51.

4. **Ye L, Haider HK, Sim EK.** Adult stem cells for cardiac repair: choice between skeletal myoblasts and bone marrow stem cells. *Exp Biol Med.* 2006; 231: 8–19.

5. **Hristov M, Heussen N, Schober A, Weber C.** Intracoronary infusion of autologous bone marrow cells and left ventricular function after acute myocardial infarction: a meta-analysis. *J Cell Mol Med.* 2006; 10: 727–33.

6. **Leobon B, Garcin I, Menaschè P, Vilquin J-T, Audinat E, Charpak S.** Myoblasts transplanted into rat infarcted myocardium are functionally isolated from their host. *Proc Natl Acad Sci USA.* 2003; 100: 7808–11.

7. **Caplice NM.** The future of cell therapy for acute myocardial infarction. *Nature.* 2006; 3: S129–32.

8. **Gnecchi M, He H, Noiseux N, Liang OD, Zhan L, Morello F, Mu H, Melo L, Pratt RE, Inwall JS, Dzau VJ.** Evidence supporting paracrine hypothesis for Akt-modified mesenchymal stem cell-mediated cardiac protection and functional improvement. *FASEB J.* 2006; 20: 661–9.

9. **Berry MF, Engler AJ, Woo YJ, Pirolli TJ, Bish LT, Jayasankar V, Morine KJ, Gardner TJ, Discher DE, Sweeney HL.** Mesenchymal stem cell injection after myocardial infarction improves myocardial compliance. *Am J Physiol Heart Circ Physiol.* 2006; 290: H2196–203.

10. **Unemori EN, Pickford LB, Salles AL, Piercy CE, Grove BH, Erikson ME, Amento EP.** Relaxin induces an extracellular matrix-degrading phenotype in human lung fibroblasts *in vitro* and inhibits lung fibrosis in a murine model *in vitro. J Clin Invest.* 1996; 98: 2739–45.

11. **Bani D, Bigazzi M.** Clinical aspects and therapeutic perspectives of relaxin. *Curr Med Chem-Immunol, Endocr Metab Agents.* 2005; 5: 403–10.

12. **Conrad KP, Novak J.** Emering role of relaxin in renal and cardiovascular function. *Am J Physiol Integr Comp Physiol.* 2004; 287: R250–61.

13. **Perna AM, Masini E, Nistri S, Briganti V, Chiappini L, Stefano P, Bigazzi M, Pieroni C, Bani Sacchi T, Bani D.** Novel drug development opportunity for relaxin in acute myocardial infarction: evidences from a swine model. *FASEB J.* 2005; 19: 1525–7.

14. **Wang QD, Sjöquist PO.** Myocardial regeneration with stem cells: pharmacological possibilities for efficacy enhancement. *Pharmacol Res.* 2006; 53: 331–40.

15. **Smits PC, van Geuns RJ, Poldermans D, Bountioukos M, Onderwater EE, Lee CH, Maat AP, Serruys PW.** Catheter-based intramyocardial injection of autologous skeletal myoblasts as a primary treatment of ischemic heart failure: clinical experience with six-month follow-up. *J Am Coll Cardiol.* 2003; 42: 2063–9.

16. **Suzuki K, Murtuza B, Fukushima S, Smolenski RT, Varela-Carver A, Coppen SR, Yacoub MH.** Targeted cell delivery into infarcted rat hearts by retrograde intracoronary infusion: distribution, dynamics, and influence on cardiac function. *Circulation.* 2004; 110: 225–30.

17. **Silvertown JD, Ng J, Sato T, Summerlee AJ, Medin JA.** H2 relaxin overexpression increases *in vivo* prostate xenograft tumor growth and angiogenesis. *Int J Cancer.* 2006; 118: 62–73.

18. **Jegger D, Jeanrenaud X, Nasratullah M, Chassot PG, Mallik A, Tevaearai H, von Segesser LK, Segers P, Stergiopulos N.** Noninvasive Doppler-derived myocardial performance index in rats with myocardial infarction: validation and correlation by conductance catheter. *Am J Physiol Heart Circ Physiol.* 2006; 290: H1540–8.

19. **Tei C, Ling LH, Hodge DO.** New index of combined systolic and diastolic myocardial performance: a simple and reproducible measure of cardiac function: a study in normals and dilated cardiomyopathy. *J Cardiol.* 1995; 26: 357-66.

20. **Vandervelde S, van Luyn MJA, Harmsen MC.** Signaling factors in stem cell-mediated repair of infarcted myocardium. *J Mol Cell Cardiol.* 2005; 39: 363–76.

21. **Kato M, Dote K, Sasaki S, Goto K, Takemoto H, Habara S, Hasegawa D.** Myocardial performance index for assessment of left ventricular outcome in successfully recanalised anterior myocardial infarction. *Heart.* 2005; 91: 583–8.

22. **Uemura R, Xu M, Ahmad N, Ashraf M.** Bone marrow stem cells prevent left ventricular remodeling of ischemic heart through paracrine signaling. *Circ Res.* 2006; 98: 1414–21.

23. **Frangogiannis NG, Smith CW, Entman ML.** The inflammatory response in myocardial infarction. *Cardiovasc Res.* 2002; 53: 31–47.

24. **Orlic D, Kajstura J, Chimenti S, Limana F, Jakoniuk I, Quaini F, Nadal-Ginard B, Bodine DM, Leri A, Anversa P.** Mobilized bone marrow cells repair the infarcted heart, improving function and survival. *Proc Natl Acad Sci USA.* 2001; 98: 10344–9.

25. **Samuel CS, Du XJ, Bathgate RA, Summers RJ.** 'Relaxin' the stiffened heart and arteries: the therapeutic potential for relaxin in the treatment of cardiovascular disease. *Pharmacol Ther.* 2006; 112: 529–52.

26. **Hayashidani S, Tsutsui H, Shiomi T, Ikeuki M, Matsusaka H, Suematsu N, Wen J, Eashira K, Takeshita A.** Anti-monocyte chemoattractant protein-1 gene tharapy attenuates left ventricular remodelin and failure after experimental myocardial infarction. *Circulation.* 2003; 108: 2134–40.

27. **Unemori EN, Lewis M, Constant J, Arnold G, Grove BH, Normand J, Deshpande U, Salles A, Pickford LB, Erikson ME, Hunt TK, Huang X.** Relaxin induces vascular endothelial growth factor expression and angiogenesis selectively at wound sites. *Wound Repair Regen.* 2000; 8: 361–70.

28. **Hewitson TD, Mookerjee I, Masterson R, Zhao C, Tregear GW, Becker GJ, Samuel CS.** Endogenous relaxin is a naturally occurring modulator of experimental renal tubulointerstitial fibrosis. *Endocrinology.* 2007 148: 660–9.

29. **Vanhoutte D, Schellings M, Pinto Y, Heymans S.** Relevance of matrix metalloproteinases and their inhibitors after myocardial infarction: a temporal and spatial window. *Cardiovasc Res.* 2006; 69: 604–13.

30. **Hughes SM, Blau HM.** Migration of myoblasts across basal lamina during skeletal muscle development. *Nature.* 1990; 345: 350–3.

31. **Wainwright CL.** Matrix metalloproteinases, oxidative stress and the acute response to acute myocardial ischaemia and reperfusion. *Curr Opin Pharmacol.* 2004; 4: 132–8.

32. **Morita H, Khanal S, Rastogi S, Suzuki G, Imai M, Todor A, Sharov VJ, Goldstein S, Neill TP, Sabbah HN.** Selective matrix metalloproinase inhibition attenuates proression of left ventricular dysfunction and remodelling in dogs with chronic heart failure. *Am J Physiol Heart Circ Physiol.* 2006; 290: H2522–7.

33. **Matsumoto R, Omura T, Yoshiyama M, Hayashi T, Inamoto S, Koh KR, Ohta K, Izumi Y, Nakamura Y, Akioka K, Kitaura Y, Takeuchi K, Yoshikawa J.** Vascular endothelial growth factor-expression mesenchymal stem cell transplantation for the treatment of acute myocardial infarction. *Atheroscler Thromb Vasc Biol.* 2005; 25: 1168–73.

34. **Wang Y, Haider HK, Ahmad N, Xu M, Ge R, Ashraf M.** Combining pharmacological mobilization with intramyocardial delivery of bone marrow cells overexpressing VEGF is more effective for cardiac repair. *J Mol Cell Cardiol.* 2006; 40: 736–45.

35. **Tang YL, Zhao Q, Qin X, Shen L, Cheng L, Ge J, Phillips MI.** Paracrine action enhances the effects of autologous mesenchymal stem cell transplantation on vascular regeneration in rat model of myocardial infarctium. *Ann Thorac Surg.* 2005; 80: 229–37.